LA-UR-19-20356

Title: MIS High-Purity Uranium/Plutonium Oxide Metal Oxidation Product SCP711-56 (SSR135): Final Report

Author(s): Veirs, Douglas Kirk
Stroud, Mary Ann
Martinez, Max
Carrillo, Alex
Berg, John M.
Narlesky, Joshua Edward
Worl, Laura Ann

Intended for: Report

Issued: 2019-09-12 (rev.1)

MIS High-Purity Uranium/Plutonium Oxide Metal Oxidation Product SCP711-56 (SSR135): Final Report

Authors:

D. Kirk Veirs
Mary A. Stroud
Max A. Martinez (retired)
Alex Carrillo (retired)
John M. Berg
Joshua E. Narlesky
Laura Worl

Metal Oxidation Product SCP711-56 (SSR135): Final Report Abstract

A high-purity uranium/plutonium mixed oxide material from the Material Identification and Surveillance (MIS) Program inventory has been studied with regard to gas generation and corrosion in a storage environment. Sample SCP711-56 represents process plutonium oxides from mixed oxides at the Hanford Site, byproduct plutonium/uranium mixed oxides at the Rocky Flats Plant, Hanford Site mixed oxides at Savannah River, mixed oxides from alloy oxidation at Savannah River, scrap mixed oxides at Savannah River and plutonium/uranium oxide at Los Alamos National Laboratory that are currently stored in 3013 containers. After calcination to 950°C the material contains 17% fuel grade plutonium and 68% uranium with approximately 1.5% impurities and the remainder principally oxygen. This study followed over time the gas pressure of a sample with nominally 0.1 wt% water in a sealed container with an internal volume scaled to 1/500th of the volume of a 3013 container. Gas compositions were measured periodically over approximately 4 years. The maximum observed gas pressure was 115 kPa. The increase over the initial pressure of 83 kPa was primarily due to generation of carbon dioxide and nitrogen gases. A small amount of hydrogen was generated and oxygen was consumed. At the completion of the study, the internal components of the sealed container showed signs of corrosion, including pitting.

Contents

Figures

Tables

Introduction

The Los Alamos National Laboratory (LANL) Shelf-life Surveillance project was established under the Material Identification and Surveillance (MIS) Program to identify early indications of potential failure mechanisms in 3013 containers.[1] Samples from plutonium processes across the DOE complex were sent to LANL to be included in the MIS inventory.[2] The small-scale surveillance project is designed to provide gas generation and corrosion information of these MIS "represented" materials under worst-case moisture loadings. This information, in combination with material characterization, allows predictions of the behavior of 3013 packaged materials stored at DOE sites. Pressure and gas compositions were monitored in small-scale reactors (SSRs) charged with nominally 10-gram samples of these plutonium or plutonium/uranium bearing "represented" materials with nominally 0.5 wt% water, the upper limit allowed by the DOE's 3013 Standard.[1] Corrosion was evaluated at the end of the study time. This report discusses sample SCP711-56 (SSR135), a high-purity mixed oxide material from the MIS Program inventory that originated at LANL via oxidation of fuel pellets on a hot plate. Sample SCP711-56 is representative of oxides generated from the following processes: [2]

- high-purity mixed oxides at the Hanford Site,
- byproduct plutonium/uranium mixed oxides at the Rocky Flats Plant, later known as the Rocky Flats Environmental Technology Site (RFETS),
- Hanford Site mixed oxides at Savannah River Site (SRS),
- mixed oxides from alloy oxidation at SRS,
- scrap mixed oxides at SRS and
- plutonium/uranium oxide at LANL

Two samples (SCP711-56A and B) were split from the original sample. These samples as-received (AR) are shown in Figure 1.

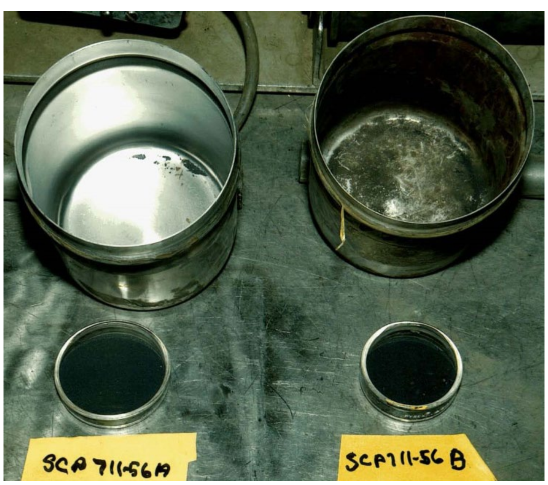

Figure 1. SCP711-56A and B upon arrival.

Material Characterization

Part of the fuels grade plutonium-uranium oxide[a] sample, SCP711-56A, was calcined at 950°C for 2 hours on July 30, 2001. Several measurements of material characteristics for the AR and calcined material are summarized in Table 1. The decrease in pycnometer density upon calcinatin is due to the formation of U_3O_8 from the oxidation of UO_2. This will be discussed later.

Table 1. Material Physical Characteristics

	Calcined	AR
Specific Surface Area (SSA) 5-point (m^2 g^{-1})	0.24	
Bulk Density (g cm^{-3})	2.94	
Tap Density (g cm^{-3})	3.98	
Pycnometer Density (g cm^{-3})	8.37	10.6

Table 2 summarizes the wt% of key elements as well as any impurity present as 0.01 wt% or greater for the As Received (AR) material. No elemental data was obtained on the calcined sample. Oxygen is not measured and it is assumed to make up the difference between the sum of the listed elements plus plutonium/uranium and 100%. No measurements of soluble species were conducted for this material. The actinide content from analytical chemistry and calorimetry/gamma isotopics is listed in Table 3.

Table 2. Elemental data obtained from atomic emission spectroscopy (AES), mass spectrometry (MS) and ion chromatography (IC).

Element	**wt% (AR)**
Aluminum	0.0888 (AES)
Calcium	0.0916 (AES)
Carbon	0.41 (MS)
Chloride	0.011 (IC)
Boron	0.0375 (MS)
Iron	0.0494 (AES)
Magnesium	0.023 (AES)
Nickel	0.1940 (AES)
Potassium	0.0369 (AES)
Silicon	0.6710 (AES)
Sodium	0.2770 (AES)

[a] The DOE defines weapons grade plutonium as plutonium containing less than 7% Pu-240. Fuels grade contains 7-19% Pu-240, and reactor grade plutonium contains greater than 19% Pu-240.

Table 3. Actinide content. For plutonium isotopes and americium, isotopic data are listed as mass fraction (g/g plutonium). The wt% uranium was determined from the Davies Gray assay method on the AR sample. Specific power is reported in mW per gram of material, not per gram of plutonium. The isotopics and specific power were measured on 12/1/2003 by calorimetry/gamma.

Isotope	Mass Fraction (g/gPu)
Pu-238	0.0005028
Pu-239	0.8863282
Pu-240	0.1090012
Pu-241	0.0039477
Pu-242	0.0002200
Am-241	0.0072478

wt% Plutonium (calorimetry) (g Pu/g of material*100)	17.2
wt% Uranium (Davies Gray)	65.7
U-234	0.008
U-235	0.717
U-236	0.002
U-238	0.273
Specific Power (mW/g of material)	0.621

The % actinide of the calcined sample (Pu% + U% +Am%) is estimated to be 83.7%. The isotopic composition of the uranium in the AR sample was 71.7% U-235 and 27.3% U-238. The material gained weight upon calcination at 950°C for 2 hours. The weight gain was 1.70%. Loss on Ignition (LOI), the weight change after the material is heated to 1000°C for 2 hours, was obtained on two AR samples. Results were 1.31 and 3.84 wt% gain, an average 2.6 wt% gain.

The stoichiometry of the uranium oxide after calcination is important to understanding the experimental observations. Water is adsorbed by UO_3 to form a dihydrate whereas UO_2 and U_3O_8 adsorb water only on the surface resulting in much lower water adsorption.[3] The stoichiometry U_3O_8 is formed from both UO_2 and UO_3 when uranium oxides are heated in air above 700°C.[3a, 4] It has been reported that some UO_3 dihydrate is formed from U_3O_8 when stored in humid, room temperature atmosphers for long times.[4] In addition, the UO_3 dihydrate appears to have a higher H_2 yield (x10) than U_3O_8 when equivalent amounts of water are present.

An attempt was made to obtain a mass balance that was consistent with (1) the reported actinide content and impurities for the AR material, (2) the weight gain upon calcination (assuming $UO_2 \rightarrow U_3O_8$), (3) the measured plutonium fraction for the calcined material, and (4) the pycnometer densities of the AR and calcined materials. A self-consistent composition was obtained in which (1) the carbon impurity was burned out upon calcination, (2) the amount of impurities was increased by 5% above their initial value, and (3) the amount of uranium was decreased by 5% below its initial value. This compostion reproduced the mass gain and density after calcination, but the density of the AR material was 12% too low. By adjusting the amount of impurities, a self-consistent result that included a small amount of UO_3 could also be obtained. We conclude that the uncertainties in the reported composition, mass gain upon heating, and densities preclude any meaningful estimate of the partition of the uranium between U_3O_8 and UO_3 in the calcined material, but small amounts of UO_3 are possible after storage in humid atmospheres.

The specific wattage of SCP711-56A as a function of time from the measurement date is shown in Figure 2.

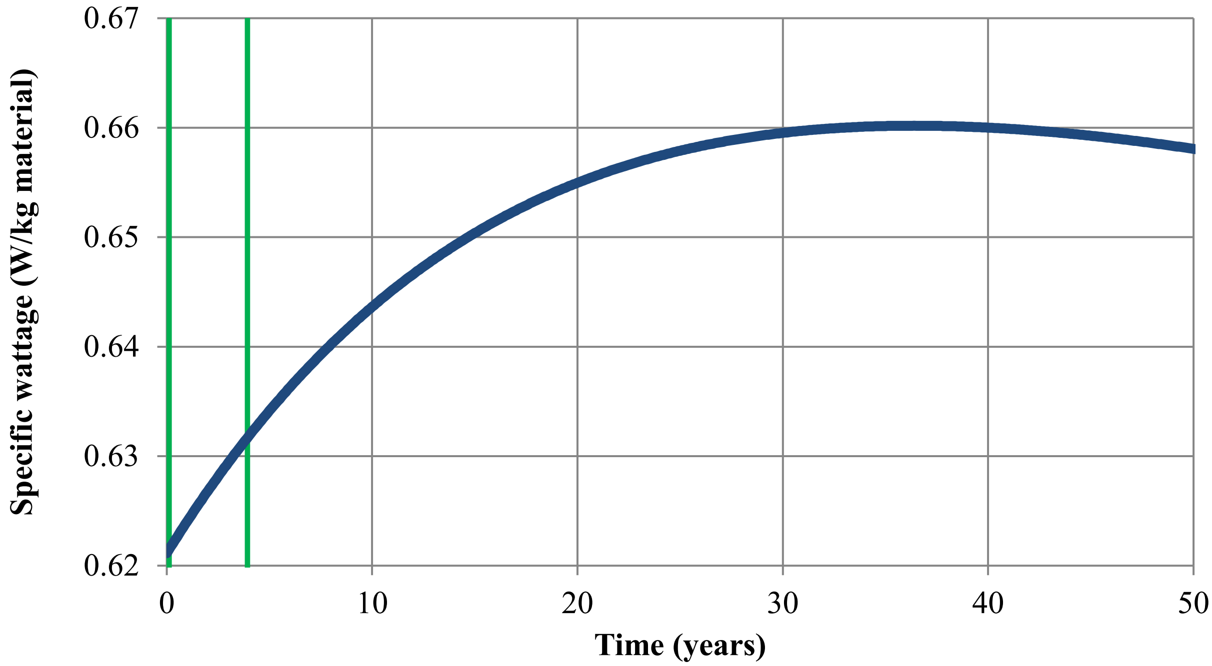

Figure 2. The specific wattage of SCP711-56A as a function of time from the last measurement date in 2003. The vertical green lines bound the time the sample was in the reactor.

Figure 3 provides information on He evolution as a function of time in SCP711-56A.

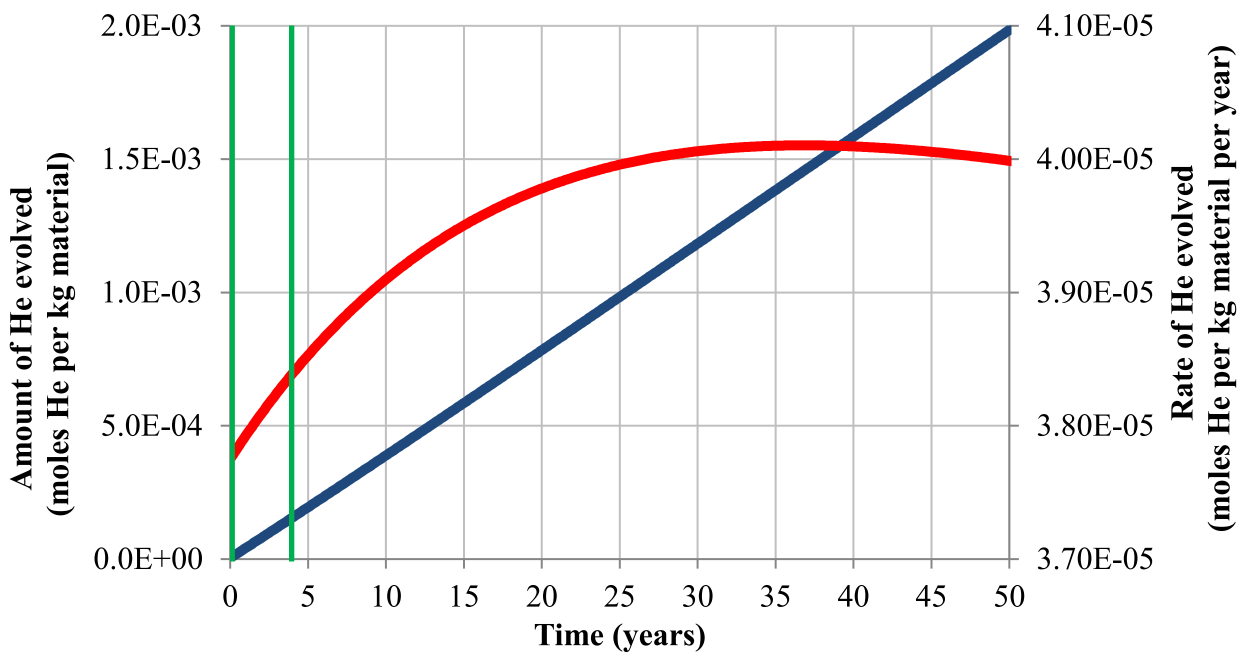

Figure 3. Integrated amount of He evolved from alpha decay as a function of time (blue line and left axis) and the moles of He per kg material evolved per year as a function of time (red line and right axis). The vertical green lines bound the time the sample was in the reactor.

Experimental Procedure

The design of the small-scale reactor (SSR) system has been described previously.[5] The container's nominally five cm^3 internal volume is scaled to ~1/500th of the inner 3013 storage container. The material of construction of the inner small-scale containers is 304L stainless steel. The SSR consists of a container body welded into a Conflat flange and a lid consisting of a Conflat flange with tubing attachments for connections to a pressure transducer and a gas manifold. An inner bucket is used to hold material and is inserted into the container body during the loading activities. The inner bucket allows the fine plutonium oxide powder to be handled with minimal or no spillage. A low-internal-volume pressure transducer and associated low-volume tubing is attached to the lid. Small-scale reactors have interchangeable parts with varying volumes. For this study, a Type H container with a total internal volume of 5.326 cm^3 was used.[6] The gas sampling volume located between two sampling valves, 0.05 cm^3 (~1 % of the SSR volume), allows gas composition to be determined with minimal effect on the internal gas pressure. A disassembled SSR is shown in Figure 4.

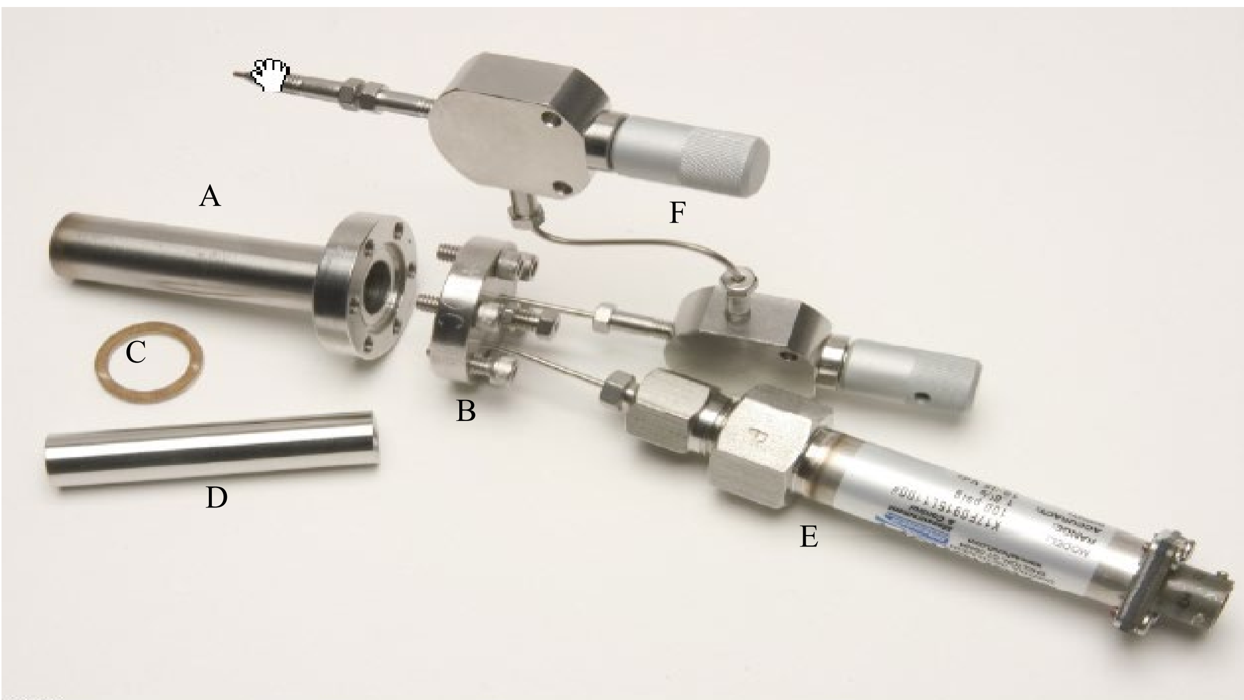

Figure 4. Dissassembled SSR: Conflat container body (A) with conflat flange lid (B), gold-plated copper gasket (C), inner bucket (D), pressure transducer (E), and a sampling volume between two sampling valves with connection to the gas manifold (F). Inner bucket slides into container body and holds the mateterial.

Gas generation is to be characterized for each MIS represented material at the bounding moisture content of 0.5 wt%. The procedure to achieve 0.5 wt% moisture included (1) estimating the moisture content of the material as it was received for small-scale loading and (2) adding sufficient water to bring the total to 0.5 wt%. The moisture content of the material was estimated by weight loss upon heating to 200°C (LOI-200°C) of a one gram sample that was cut from the parent lot at the same time as the 10 g small-scale sample. The LOI-200°C samples were placed in a glass vial which remained in the glove box line with the small-scale sample until the LOI-200°C measurement was performed, typically one day or less after the sample split and just prior to SSR loading. LOI-200°C involved heating nominally one gram of the material for 2 hours at 200°C, cooling the material for 10 minutes and determining the mass difference of the material before and after heating. The mass loss observed was attributed to adsorbed water. It was assumed that the LOI-200°C material contained an additional ~1.5 monolayer equivalent of water, approximately 0.01 wt% for this material, as hydroxyls or chemically adsorbed water which was not removed by heating to 200°C.[7] The amount of water to be added to achieve 0.5 wt% total moisture was calculated as the difference between 0.5 wt% and the mass loss by LOI-200°C. No estimate of chemically adsorbed water was included in the sum to 0.5 wt%. In addition, a sample from the parent was split and placed in a glass vial inside of a hermetically sealed container. The water content of this sample was determined by Thermal Gravametric Analysis-Mass Spectroscopy. TGA-MS is inherently more accurate than LOI-200°C, although there can be errors associated with this method due to handling and excessive times before the sample is run. TGA-MS results were not available at the time of loading.

The procedure to add moisture is described briefly. A ten-gram sample of the SCP711-56A material was placed on a balance in a humidified chamber. Weight gain was recorded as a function of time. The sample was then placed into a small-scale reactor. The glove boxes used for loading and surveillance were flushed with He, resulting in a glove box atmosphere of mainly He with a small amount of air. Some moisture loss was expected during transfer from the humidified chamber into the SSR in the very dry glove box atmosphere (relative humidity < 0.1 %). Transfer time from the balance where the final mass measurement is made to when the SSR was sealed was kept to approximately 45 seconds. Weight loss during transfer for high-purity oxides was measured to be 0.07 wt% per minute.[8] This correction, 0.05 wt%, was applied to obtain the estimated moisture content. In this case, the desired 0.5 wt% total moisture was not achieved because the sample did not pick up sufficient moisture from the humidified atmosphere as described in the Results section.

The sealed SSR was placed in a heated sample array maintained at 55°C. Fifty microliter gas samples were extracted through a gas mainfold. Fifty microliters corresponds to 1.2% of the free gas volume. The gas sample was analyzed using an Agilent 5890 GC (gas chromatograph) calibrated for He, H_2, N_2, O_2, CO_2, CO and N_2O. Water vapor was not measured in these samples. The pressure and array temperature was recorded every fifteen minutes. The pressure data was reduced to weekly average values reported here. Gas composition was sampled at least annually.

At the termination of the experiment, a final GC gas sample was taken, and the SSR was removed from the array and allowed to cool to glove box temperature. The SSR lid was removed and a new lid containing a relative humidity sensor was placed on the container within 20 seconds of removal. After allowing 53 minutes for the system to equilibrate, the relative humidity and temperature in the container were measured using a Vaisala HMT330 sensor and readout. The material was then removed from the container and the moisture content in the material was determined by performing LOI-200°C.

Results

Loading

A ten-gram split from the parent was selected for loading into the SSR. The mass of the sample prior to moisture loading, m_{mat}, the volume the material occupies calculated from m_{mat} and the pycnometer density, V_{mat}, and the calculated free gas volume within the SSR, V_{gas}, during the gas generation study are given in Table 4.

Table 4. Mass of sample and results of calculation of free gas volume using approach in Reference 8.

Mass of sample m_{mat}	Volume of Material V_{mat}	Volume of SSR V_{SSR}	Free Gas Volume in SSR V_{gas}
10.00 g	1.195 cm^3	5.326 cm^3	4.131 cm^3

TGA-MS Results

TGA-MS data for the sample of the parent material are shown in Figure 5. The sample was large enough to split into three subsamples. TGA traces for all three subsamples and MS traces for channels that were above background for one of the three samples are illustrated. Total moisture content was determined to be 0.043 wt% to 950°C. During the TGA-MS analysis, 0.054 wt% carbon dioxide and 0.0160 wt% nitrogen oxide was released. The LOI-200°C loss of 0.08 wt% overestimates the amount of water for this material, which had been exposed to air for 2.4 years prior to the measurement. The presence of surface adsorbed nitrogen oxide species and CO_2 on aged material limits the accuracy of the LOI-200°C techniques to estimate water content.

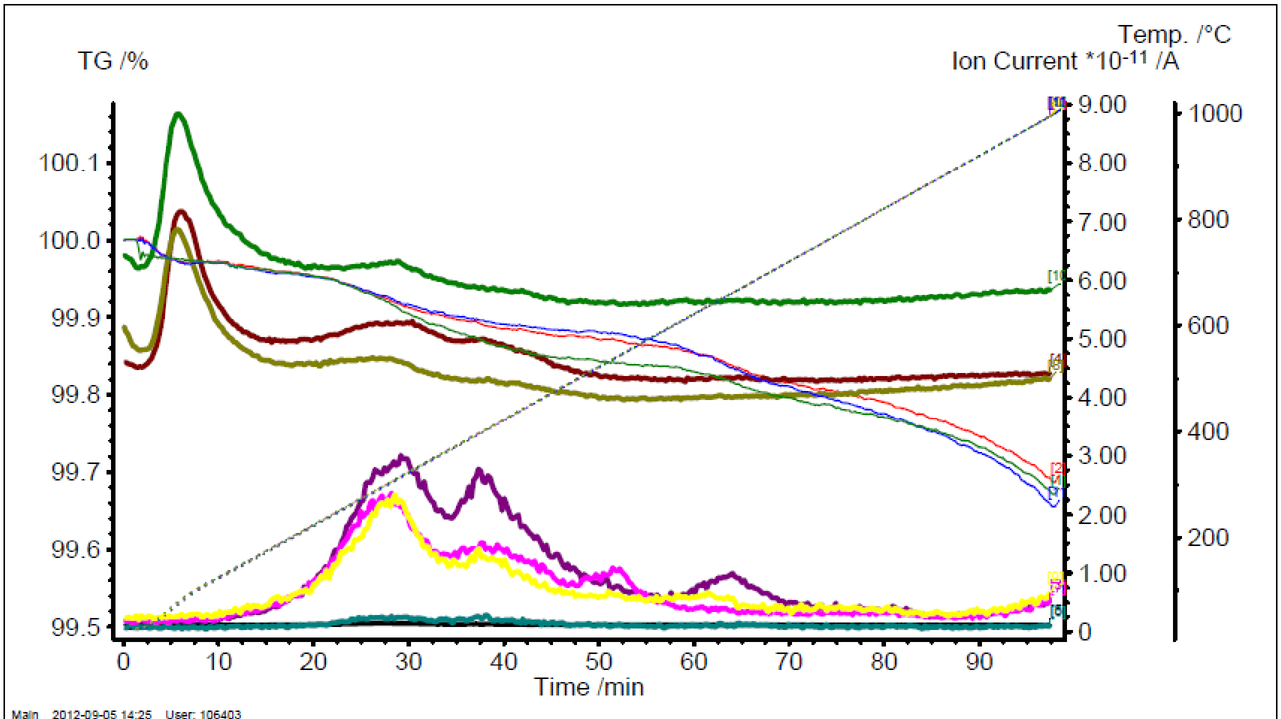

[#] Instrument	File	Date	Identity	Sample	Mass/mg	Segment	Range	Atmosphere	Corr.
[1] STA 409 PC/PG	135s1_030804a.dsv	2004-03-08	135s1_030804a	Buoyancy	300.000	1/1	20.0/10.0(K/min)/1000.0	Argon/45/15prot/60pur / ---/--- / ---/---	TG:020
[2] STA 409 PC/PG	135s2_030904a.dsv	2004-03-09	135s2_030904a	Buoyancy	300.000	1/1	20.0/10.0(K/min)/1000.0	Argon/45/15prot/60pur / ---/--- / ---/---	TG:020
[3] Balzers MID	135s1_m44.00.imp	2004-03-08	135s1	Mass 44.00		1/1	29/9.9(K/min)/994		---
[4] Balzers MID	135s1_m17.00.imp	2004-03-08	135s1	Mass 17.00		1/1	29/9.9(K/min)/994		---
[5] Balzers MID	135s1_m46.00.imp	2004-03-08	135s1	Mass 46.00		1/1	29/9.9(K/min)/994		---
[6] Balzers MID	135s1_m12.00.imp	2004-03-08	135s1	Mass 12.00		1/1	29/9.9(K/min)/994		---
[7] Balzers MID	135s2_m44.00.imp	2004-03-09	135s2	Mass 44.00		1/1	27/9.9(K/min)/994		---
[8] Balzers MID	135s2_m17.00.imp	2004-03-09	135s2	Mass 17.00		1/1	27/9.9(K/min)/994		---
[9] Balzers MID	135s3_m44.00.imp	2004-03-11	135s3	Mass 44.00		1/1	28/9.9(K/min)/994		---
[10] Balzers MID	135s3_m17.00.imp	2004-03-11	135s3	Mass 17.00		1/1	28/9.9(K/min)/994		---
[11] STA 409 PC/PG	135s3_031104a.dsv	2004-03-11	135s3_031104a	Buoyancy	300.000	1/1	20.0/10.0(K/min)/1000.0	Argon/45/15prot/60pur / ---/--- / ---/---	TG:020

Figure 5. TGA-MS data for the parent material. Mass 17.00 is H_2O, and Mass 44 is CO_2.

Moisture addition

The measurements and assumptions used to calculate the moisture content at the time of loading are summarized in Table 5. The best value for the moisture content at loading is 0.06 wt% as given in Table 5 line 12, Estimated Total Moisture in loaded sample (using TGA-MS).

Table 5. Moisture data summary at loading for SSR135

	Parameter	Value	Units
1	Original Calcination Date	7/30/2001	
2	Loading Date	1/12/2004	
3	Unloading Date	11/5/2007	
4	Initial sample weight (m_{mat})	10.00	g
5	Initial Moisture (Total) by TGA-MS	0.04	wt%
6	Initial Moisture by LOI-200 °C	0.08	wt%
7	Total Moisture added	0.07	wt%
8	Relative Humidity in glove box during loading	0.1	%
9	Estimated moisture loss during loading	0.05	wt%
10	Estimated **Total Moisture** in loaded sample (using LOI) = Line 6 +Line7 –Line 9	0.10	wt%
11	Estimated **Total Moisture** in loaded sample (using TGA-MS) = Line 5 + Line 7 –Line 9	0.06	

The moisture uptake as a function of exposure time to a high humidity atmosphere is plotted in Figure 6. Moisture addition was discontinued on this very low SSA material after 20 hours because of the very slow (possibly reversing) moisture uptake. The increase in mass is attributed to water adsorption by the material. Some loss of water occurs when the material is transferred from the humidified chamber to the balance where the final mass measurement is made. Thus, the total moisture added in Table 5, 0.07 wt%, is 0.05 wt% less than the mass gain during moisture uptake, 0.12 wt%.

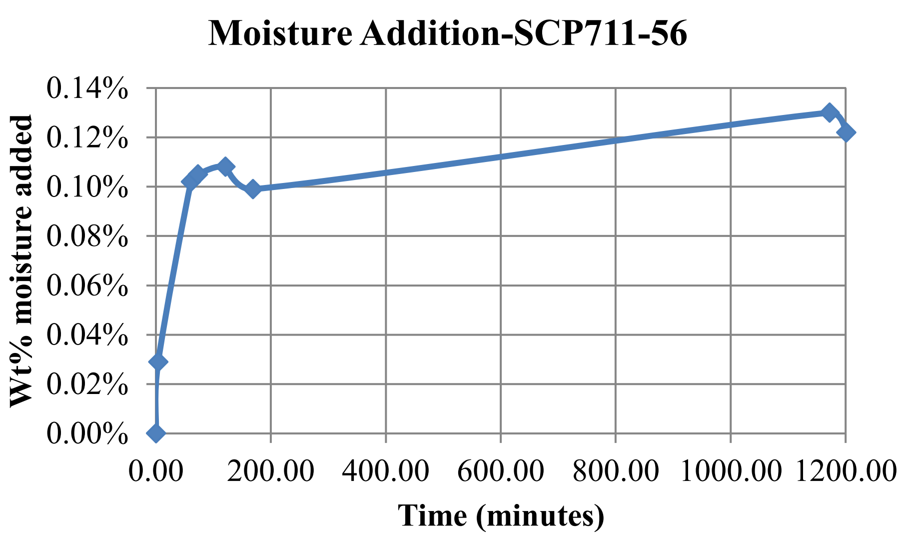

Figure 6. Moisture Addition Curve

Gas Generation

The total pressure in SSR135 as a function of time, as well as the partial pressure of several gases, is shown in Figure 7. Pressures reflect changes in the gases in the reactor as well the 1.2% pressure drop due to gas sampling. Detailed information on gas composition and uncertainties is in Attachment 1 and on pressure in Attachment 2.

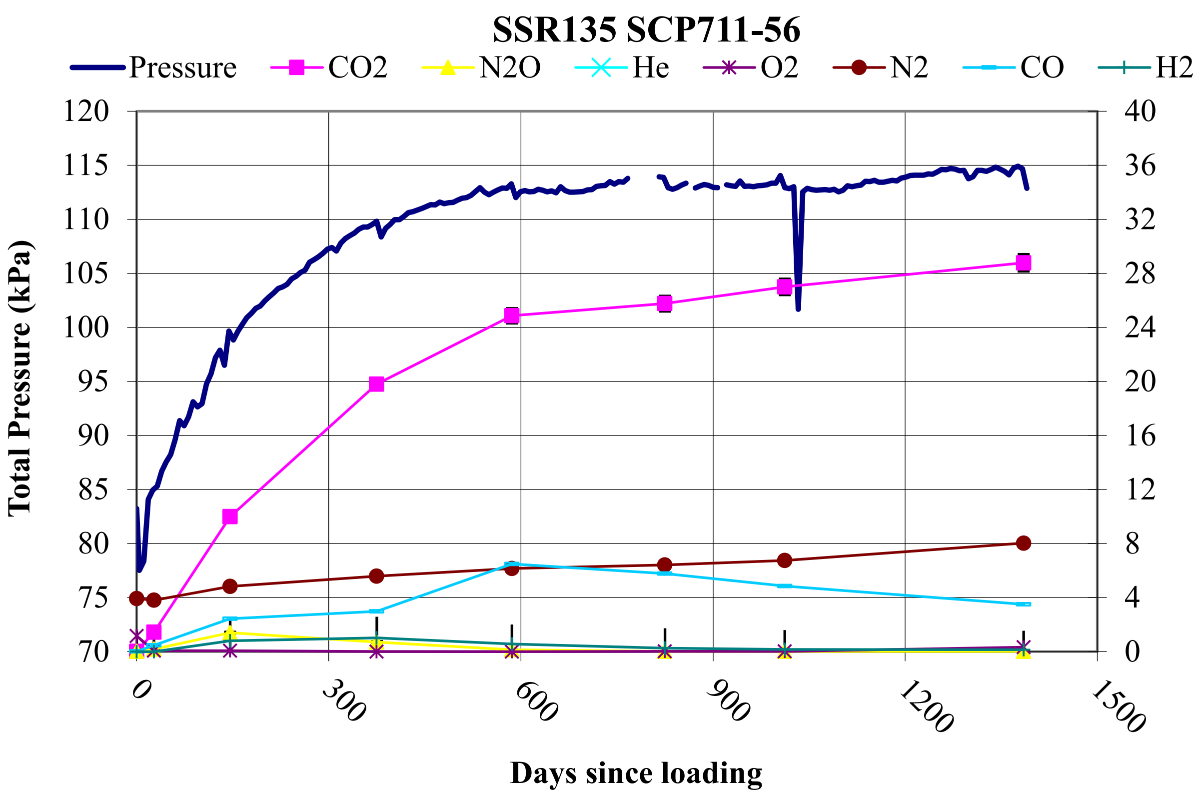

Figure 7. Total pressure and partial pressure of gases measured using a gas chromatograph as a function of time. He and Total pressure is plotted on the left total pressure scale.

The initial pressure of 83 kPa increased to 100 kPa in the first five months and gradually increased to a maximum pressure of 115 kPa over the next 3.5 years. Hydrogen and oxygen were minor components in the headspace gas. Hydrogen was initially not detected and increased to 1 kPa after one year after which the hydrogen pressure gradually decreases, reaching 0.1 kPa at termination. Oxygen began at 1.2 kPa and decreased to 0.1 kPa within a month. The 0.3 kPa detected in the final measurement may have been due to insufficient pump down during sampling.

The net increase in total pressure during the experiment was primarily due to the generation of carbon dioxide which increased to 29 kPa. N_2 reached a maximum value of 8 kPa and CO reached 6.5 kPa. The CO and CO_2 behavior is similar to that observed in two previous small scale studies on high-purity oxides (TS70701 and 5501579), however they generated nearly 50 kPa of N_2 as well.

Moisture measurements on unloading

The SSR was removed from the heated array and placed in a holder to cool. After two days, the lid was removed and it was replaced with a lid modified to hold a RH sensor. The relative humidity and temperature in the container were measured using a Vaisala HMT330 sensor and readout. The weight loss in the material at termination by performing LOI-200°C was 0.03 wt%. To estimate the total moisture at unloading, an additional 0.008 wt% (1.5 ML) was added to estimate the chemically adsorbed water not removed by heating to 200°C.

The unloading LOI-200°C (0.03 wt%), was 0.05 wt% less than the LOI-200°C (0.08 wt%) at loading. Some of the original carbon and nitrogen surface species were lost to the gas phase as CO_2, CO, and N_2 and are quantified in the discussion. Differences in the amount of other gases desorbing from the initial and final sample could account for some of the difference in the LOI.

Given the measured RH of 1.4% at 23.8°C in the SSR at unloading, BET theory predicts ~ 0.1 ML or 0.0005 wt% physisorbed water was present and assuming 1.5 ML (0.008 wt%) present as chemisorbed water, the RH estimate of the moisture at unloading is 0.009 wt%. (See Appendix 3).

Sample unloading and moisture data are summarized in Table 6.

Table 6. Unloading moisture data summary

	Parameter	Value	Units
1	Unloading moisture by LOI-200 °C	0.035	wt%
2	Estimated additional strongly bound moisture of 1.5 ML	0.008	wt%
3	Estimated **Total Moisture** at unloading from LOI = Line 1 + Line 2	0.042	wt%
4	Relative Humidity/Temperature in headspace at unloading	1.4 / 23.8	%/ °C
5	Number of monolayers at unloading RH and temperature using Figure A-1 and c=7.	0.1	ML
6	Mass of weakly bound water (RH) using # of MLs in line 5.	0.00053	wt%
7	Estimated **Total Moisture** at unloading from RH = line 2 + line 6	0.0085	wt%

Corrosion

Images of the inner bucket after unloading are shown in Figure 8. No images of the outside of the inner bucket are available.

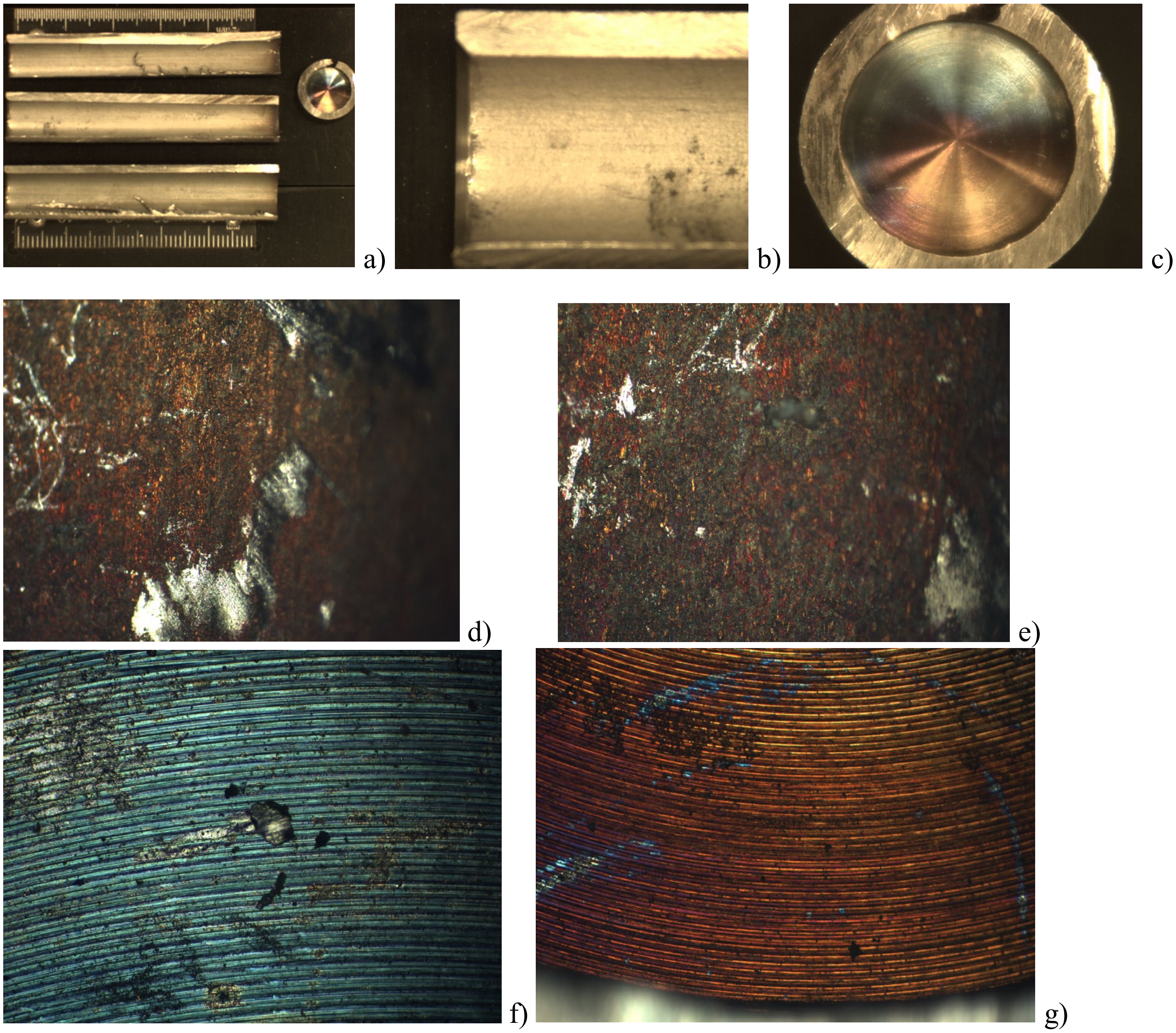

Figure 8. Photographs after unloading: a) inner bucket b) wall of inner bucket c) bottom of bucket. Micrographs after unloading: d) & e) corrosion of inner wall showing red coloring inherent of corrosion of Fe f) and g) corrosion of bottom of bucket, showing pitting.

Corrosion was observed within SSR135 which is unexpected because the material is high-purity plutonium-uranium oxide with only trace amounts of chlorine. A rust colored coating was observed on the inner wall and bottom and pitting was observed on the bottom of the bucket.

Discussion

A goal of the small-scale surveillance studies is to understand the hydrogen gas generation response of material exposed to moisture over a broad range of materials. Recommendations on the analysis of hydrogen partial pressure curves include calculations to obtain hydrogen G-values and formation and consumption rate constants assuming that the hydrogen gas is formed either from radiolysis or from surface reactions with water.[6] In order to perform these calculations, knowledge of the moisture content of the material during the study and the dose to the moisture is required. We will first discuss the amount of moisture on the material during the study and use the results as input to the $G(H_2)$ and rate constant calculations. We will follow those results with a discussion of the observation of other gases.

Unlike plutonium-bearing materials currently stored in 3013 containers throughout the DOE complex, SCP711-56 was exposed to air for 2.5 years after calcination prior to loading. A significant formation of hydroxyls on the oxide surface is expected after this much time, although with a low SSA hydroxyl formation represents less than 0.01 wt%. Gases, such as CO_2 or NOx, would also be adsorbed to the surface and come off of the material when moisture is added to the system. The presence of these species may alter the gas generation behavior compared with recently calcined (to 950°C) plutonium/uranium oxide.

When U_3O_8 is stored under high RH conditions near 90%, $UO_3{\cdot}2.25H_2O$ and $UO_3{\cdot}2H_2O$ are formed within 3.5 years.[3b] The calcined material was stored in the vault at a lower RH, probably near 30% (ranged from 17 -34% depending on the room). It would be reasonable that the calcined material after 2.5 years in the vault contained some hydrated UO_3. Generation of a small amount of H_2 and, in particular, the low RH at unloading, suggests a hydrated UO_3 is present. The amount of weakly bound water on the sample at unload from LOI, 0.035 wt%, was seven times larger than that expected from the 1.4% RH measurement at unload (0.0005 wt% physically bound water on the surface from BET theory.) This suggests the additional water is chemically bound in a hydrated compound, making minimal contribution to the RH in the container. Studies of water associated with U_3O_8 and UO_3 exposed to gamma radiation show that water associated with UO_3 generates H_2 at x10 the rate of water associated with U_3O_8, but less than water that is 10 monolayers thick on an oxide surface.[3a, 9] If $UO_3{\cdot}2H_2O$ is the species responsible for the water that is not physically adsorbed on the surface, then the amount of UO_3 present would be 0.3 wt%. The presence of $UO_3{\cdot}2H_2O$ would explain the amount of water at unloading which is hard to explain with an oxide with only 0.24 $m^2\ g^{-1}$ SSA, and the small amount of H_2 generated.

H_2 G-value and rate constants

The formation and consumption of H_2 can be represented in a simple scheme as:

$$H_2O \overset{k_1}{\rightarrow} H_2 + 1/2O_2 \qquad \text{Equation 1}$$

$$H_2 + 2PuO_2 \overset{k_2}{\rightarrow} 2\ PuOOH \qquad \text{Equation 2}$$

where the oxygen in Equation 1 either enters the gas phase or is consumed by the PuO_2. The oxygen does not appear to affect the behavior of the hydrogen. Less than 1 kPa of oxygen gas was observed and it was subsequently consumed so both mechanisms probably occurred. The material present within the sealed container that has the greatest potential to consume H_2 is PuO_2. The precise nature of the formation and consumption reactions are not known and the product shown in Equation 2 is for illustration purposes. The important aspect of Equation 2 is that the H_2 forms a species that does not reform H_2O.

The change in H_2 pressure due to the reactions in Equation 1 and Equation 2 can be written in differential form as:

$$\frac{dP_{H2}}{dt} = k_1\ A(t) - k_2 P_{H2} \qquad \text{Equation 3}$$

where P_{H2} is the partial pressure of hydrogen, A(t) is the active water in the reactor involved in hydrogen generation, expressed in units of pressure using the ideal gas law, t is time in days, and k_1 and k_2 are the first-order rate constants for the formation and consumption of hydrogen in $days^{-1}$. The model assumes exponential decay of the active water, A(t), with time as shown in Equation 4.

$$A_{H_2O}(t) = A_0 e^{-k_1 t} \qquad \text{Equation 4}$$

where A_0 is the amount of active water at t=0. Substituting Equation 4 into Equation 3 yields Equation 5:

$$\frac{dP_{H2}}{dt} = k_1\ A_0 e^{-k_1 t} - k_2 P_{H2} \qquad \text{Equation 5}$$

The initial rate of hydrogen generation is calculated by evaluating Equation 5 at t = 0 assuming P_{H_2} is zero at t=0. The initial rate is equal to k_1A_0 (Appendix 3.)

Equation 5 can be integrated to yield the following, again assuming P_{H_2} is zero at t=0.

$$P_{H_2}(t) = \frac{A_0 k_1}{k_2 - k_1}\left(e^{-k_1 t} - e^{-k_2 t}\right) \qquad \text{Equation 6}$$

The maximum hydrogen pressure is calculated from Equation 7 where K = k_2/k_1.

$$P_{max} = A_0\left(K^{K/(1-K)}\right) \qquad \text{Equation 7}$$

The hydrogen partial pressure versus time observations for SSR135a, fit to Equation 6, is shown in Figure 9. (Due to the known leak in the system, data from SSR135 was not fit.)

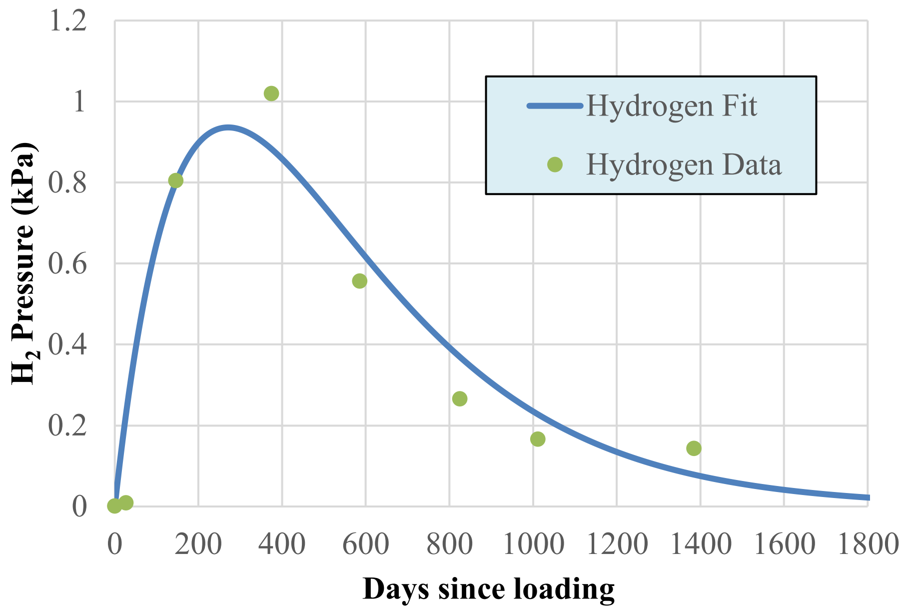

Figure 9. The hydrogen partial pressure and the fit to Equation 6, or first order formation and first order consumption reaction with an r^2 coefficient of 0.93.

The values for the fit parameters yielding the curves in Figure 9 along with the standard error in the parameters are given in Figure 7. The function reached a maximum of 0.94 kPa at 271 days. The initial rate of hydrogen generation calculated from these parameters are also reported in Table 7.

Table 7. The fit parameters, standard errors and initial rate from the hydrogen generation data for SSR135 at 55 C from Eq 6.

Small-scale Surveillance sample ID	A_0 *kPa*	k_1 (day^{-1})	k_2 (day^{-1})	*Initial Rate (kPa/day)* (k_1A_0)
SSR135	2.56	0.00367	0.00371	0.0094
Standard Error	126	0.18	0.18	

The low initial active water determined from the fit corresponds to 0.0007 wt% or approximately 1% of the initial water loaded on the sample as measured by TGA (weakly and strongly bound). The estimated wt% water active in hydrogen formation (A) remaining in the system as a function of time is plotted in Figure 10 using the Equation 4 below.

$$A(t) = A_0 e^{-k_1 t}$$

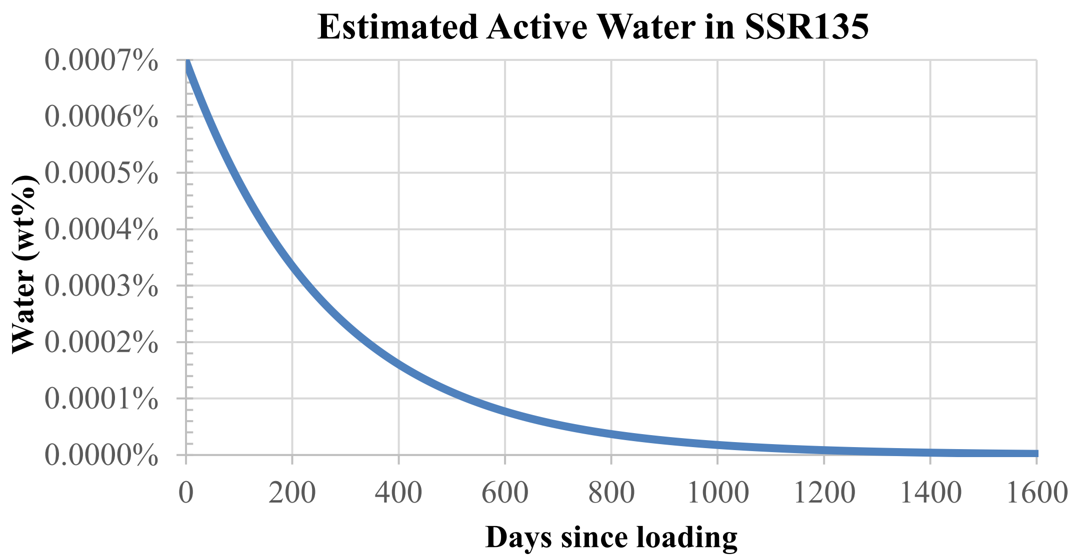

Figure 10. Graph of the estimated active water, A(t), in SSR135 as a function of time, where A_0 is expressed in terms of wt% of water.

The plot indicates that all of the initial active water reacted to form hydrogen by the termination of the experiment.

Estimation of the amount of moisture on the material during the gas generation study

SCP711-56A after calcination to 950°C contains PuO_2 and U_3O_8 with perhaps a small amount of UO_3. UO_3 picks up water and forms hydrates such as $UO_3 \cdot 2H_2O$ when exposed to moisture.[3] Moisture adsorbtion by high-purity PuO_2 and U_3O_8 is very small[3a] and the moisture is thought to exist as physisorbed water that behaves according to BET theory[10] and as chemically bound water with very low chemical activity (very low water vapor pressure). The latter water can be described as surface hydroxyls and is removed from the oxide surfaces only at high temperatures. The best estimate of the moisture at loading is 0.060 wt%. A monolayer of moisture is 0.0053 wt%, thus the amount of moisture at loading if it is all physically and chemically adsorbed onto the 0.24 $m^2\ g^{-1}$ surface represents approximately 11 monolayers. If UO_3 were present, formation of $UO_3 \cdot 2H_2O$ is likely. The water would then be partitioned as follows. At loading, 1.5 monolayers (0.0080 wt%) as hydroxyls, 0.09 monolayers physisorbed from BET using RH at unloading (0.0005 wt%), with the remainder as hydrates associated with UO_3 (0.052 wt%). At unloading, 1.5 monolayers as hydroxyls (0.008 wt%), 0.09 monolayers as physisorbed at a RH of 1.4% (0.0005 wt%), the equivalent of 2.56 kPa dissociated as H_2 (0.007 wt%), water vapor at 1.4% RH at 24 °C (0.00011 wt%), and the remainder still associated with UO_3 as hydrates (0.030 wt%). The LOI measurement at unloading includes the physisorbed monolayers and at least the first water of hydration[3a]. (For these calculations it is assumed the LOI contains all hydrates.) Table 7 summarizes the amount of water on the material, in the gas phase, and decomposed to form H_2 expressed as weight percent, moles, grams, and monolayers.

Table 8. The amount of water adsorbed on the material, in the gas phase, and decomposed to form H_2 expressed as moles, grams, and monolayers. The mass of water in a monolayer is 0.00053 g. Calculations use SSA = 0.24 m^2 g-1 ,.m_{mat} = 10.00 g and V_{gas} = 4.131 cm^3.

Water Source	**Amount of Water**			
	wt%	g	Moles	monolayers
	0.0053	0.00053	2.9×10^{-5}	1
Estimated total moisture at loading from Table 5	0.060	0.0060	0.00033	11
Water consumed to form H_2 (from fit A0= 2.56 kPa)	0.0007	7.0E-05	3.9E-06	0.13
Water vapor at unloading, 23.8 °C and 1.4% RH (0.4 kPa)	0.00011 (equivalent)	1.1E-05	6.1E-08	0.02 (equivalent)
Water as hydroxyls (1.5 ML)	0.008	.00080	4.4E-05	1.5
On material at unloading by LOI	0.030	0.0030	0.0002	5.7
Total in system at loading from unloading data = water consumed +water vapor + hydroxyls + LOI	0.039	0.0039	0.00022	7.4

(Note: Additional moisture could have been consumed in formation of the corrosion products such as iron hydroxide)

A_0, k_1, and k_2 are used to calculate *G(H_2)* and the rate constants for the hydrogen formation and consumption surface reactions using equations in Appendix 5. Because of the uncertainty in determining the amount of water involved in the hydrogen generation, several values are used for the variable m_{H2O} for comparison, the total moisture at loading, the total moisture at unloading, and the water consumed to form H_2. The stopping power ratio for SCP711-56 material, $\frac{S_{H_2O}}{S_{mat}}$, is 3.46 (Appendix 4). Results for the multiple choices of water, using equations from Appendix 5, are reported in Table 9 and 10.

Table 9. G(H2) calculated from the reaction parameters and the estimated moisture content using equation A6-4 in Appendix 6 assuming radiolytic decomposition of water to form H_2.

Water Source	***G(H2)***
	molecules $100eV^{-1}$
Estimated total moisture at loading from Table 5 (0.0060 g)	0.12
Total moisture at loading from unloading data:(0.0039 g)	0.18
Water consumed to form H_2 (7E-05 g)	10

Table 10. Rate constants calculated from the reaction parameters and the estimated moisture content assuming surface catalyzed decomposition of water to form H_2.

Variable	**Equation in Appendix 5**	**Value**	**Units**
k_{for}	A5-5	1.0E+11	molecules s-1
k_{con}	A5-6	3.9E+10	molecules s-1 kPa-1
R_{for}	A5-8	0.25	nanomoles m-2 hr-1
R_{con}	A5-9	0.098	nanomoles m-2 hr-1

Figure 11 compares the $G(H_2)$ values determined in this study with those reported previously.[12]

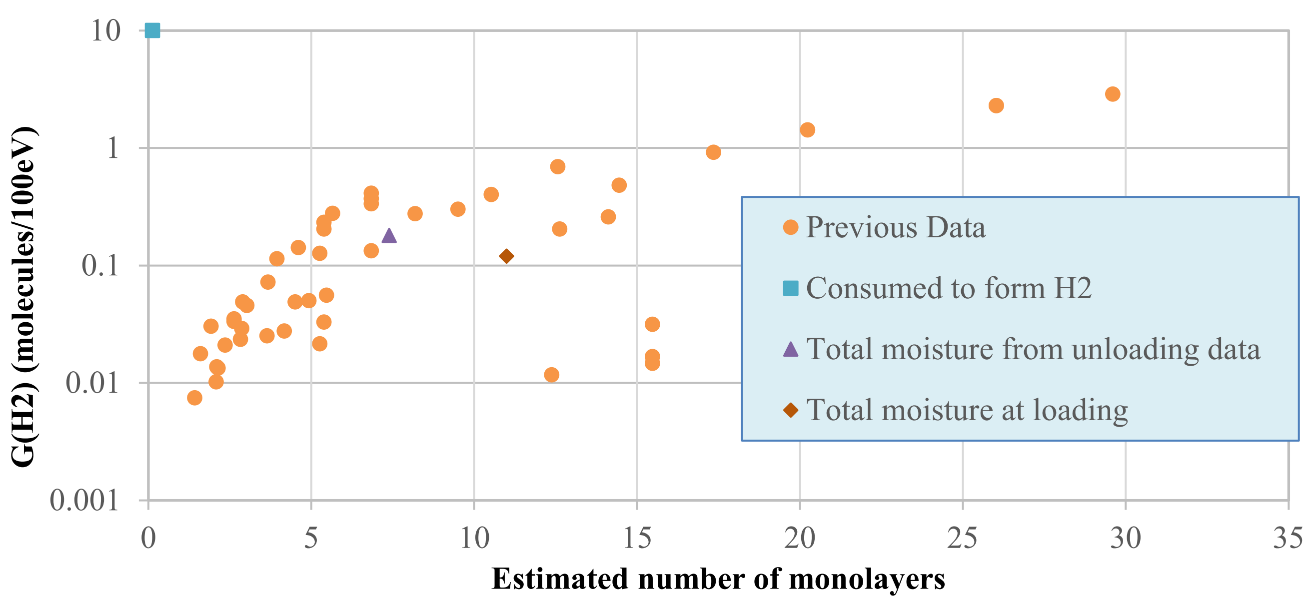

Figure 11. Comparison of calculated $G(H_2)$ plotted against the number of calculated water monolayers determined in this study with those from previous research based on no back reaction.

Behavior of CO_2 and NO_2

The carbon dioxide and nitrogen dioxide detected by TGA-MS on the 10 g sample at loading are a possible source for the CO_2 and N_2 observed in the gas phase. (The compounds actually bound to plutonium dioxide surface could have been any of the general forms COx and NOx). The number of moles of nitrogen gas and carbon dioxide present in the head space at the termination of the experiment were calculated using the ideal gas law, n = PV/RT, where V = 4.131 cm^3, T = 328 K, and P = partial pressure of the gas (P_{CO2}=29 kPa at termination and at maximum , P_{NO2}= 0 kPa at termination and 1.4 kPa at maximum and P_{N2} = 8 kPa at maximum maximum). Results are summarized in Table 10.

Table 11. Amount of nitrogen species detected on the surface prior to loading compared to the amount detected in the gas phase.

	CO_2 (moles)	NO_2 (moles)	N_2 (moles)	N (moles)
Sample (Loading-TGA-MS)	1.2×10^{-4}	3.5×10^{-5}	Not measured	3.5×10^{-5}
Head Space (Termination-GC)	4.4×10^{-5}	0	6.2×10^{-6}	1.2×10^{-5}
Max Detected in Head Space over duration of experiment (GC)	4.4×10^{-5}	2.1×10^{-6}	6.2×10^{-6}	1.5×10^{-5}

About a third of the carbon dioxide detected by TGA-MS was released, and approximately 50% of the nitrogen in the NOx gases detected by TGA-MS was released from the surface as N_2/NO_2 by the termination of the experiment. Prior to loading the sample in the small-scale reactor, the plutonium dioxide powder was exposed to air for 2.4 years (nitrogen and oxygen with small amounts of water and carbon dioxide). The sample was placed in a helium atmosphere within the small-scale reactor with a small partial pressure of water. A possible explantion for the increase in CO_2 is that the water displaced chemically adsorbed CO_2 from the surface sites. The production of N_2 from the NOx species adsorbed on the surface suggests that the reaction to form NOx from radiolysis of air is reversible in the alpha radiation environment on the surface.

Behavior of He

The alpha decay of the Pu and Am creates He, which may escape the oxide into the gas phase. The amount of He created depends upon the mass of the material and the rate of decay of the various isotopes. The rate of decay can be illustrated graphically as the specific wattage calculated from the reported isotopics, Figure 2. Results were calculated using the last reported isotopics measurements taken on December 1, 2003, that are reported in Table 3. The integrated and differential amount of He evolved as a function of time are shown in Figure 3.

The amount of He created due to alpha decay over the time the material was in the SSR is estimated to be 1.5×10^{-6} moles for the 10 g sample. This amount of He would result in a gas pressure increase of 1 kPa in the 4.131 ml of gas volume and gas temperature of 328 K, if all the He was released into the gas phase. Instead the He pressure declined by approximately 6 kPa, which is approximately the decrease expected due to the 7 gas samplings. Thus, the amount of He generated by this material is too low to be detected in this study.

Conclusions

The MIS item SCP711-56A was entered into surveillance in December of 2003 and removed from surveillance in March of 2010. The amount of water on the material during the gas generation study was estimated to be 0.06 wt%. The gas generation was dominated by CO_2 with some N_2. Hydrogen was generated to a maximum partial pressure of 1.0 kPa. The oxygen that was initially present (1.2 kPa) was mainly consumed. Corrosion was observed on the wall and bottom of the inner bucket.

Acknowledgements

Funding for this work was provided to the MIS Program by the Assistant Manager for Nuclear Materials Stabilization, Savannah River Operations Office, Department of Energy's Office of Environmental Management. The authors acknowledge Luke Simms and Holden Hyer for assistance with data compilation.

References

1. Department of Energy, Stabilization, Packaging, and Storage of Plutonium-Bearing Materials. U.S. Department of Energy: Washington, D.C. 20585, 2012.
2. Narlesky, J. E. P., L. G.; Friday, G. P. *Complex-Wide Representation of Material Packaged in 3013 Containers*; LA-UR-14396; Los Alamos National Laboratory: Los Alamos, NM, 2009.
3. (a) Icenhour, A. S.; Toth, L. M.; Luo, H. *Water Sorption and Gamma Radiolysis Studies for Uranium Oxides*; ORNL/TM-2001/59; Oak Ridge National Laboratory: Oak Ridge, TN, 2002; (b) Tamasi, A. L.; Boland, K. S.; Czerwinski, K.; Ellis, J. K.; Kozimor, S. A.; Martin, R. L.; Pugmire, A. L.; Reilly, D.; Scott, B. L.; Sutton, A. D.; Wagner, G. L.; Walensky, J. R.; Wilkerson, M. P., Oxidation and Hydration of U3O8 Materials Following Controlled Exposure to Temperature and Humidity. *Analytical Chemistry* **2015,** *87* (8), 4210-4217.
4. Thein, S. M.; Bereolos, P. J. *Thermal Stabilization of* $^{233}UO_2$, $^{233}UO_3$, *and* $^{233}U_3O_8$; ORNL/TM-2000/82; Oak Ridge National Laboratory: Oak Ridge, TN, 2000.
5. Veirs, D. K.; Worl, L. A.; Harradine, D. M.; Martinez, M. A.; Lillard, S.; Schwartz, D. S.; Puglisi, C. V.; Padilla, D. D.; Carrillo, A.; McInroy, R. E.; Montoya, A. R. *Gas generation and corrosion in salt-containing impure plutonium oxide materials: Initial results for ARF-102-85-223*; LA-UR-04-1788; Los Alamos National Laboratory: Los Alamos, NM, 2004.
6. Veirs, D. K.; Berg, J. M.; Stroud, M. A. *Obtaining G-values and rate constants from MIS data*; LA-UR-17-23787; Los Alamos National Laboratory: Los Alamos, NM, 2017.
7. Veirs, D. K.; Berg, J. M.; Crowder, M. L. *The effect of plutonium dioxide water surface coverage on the generation of hydrogen and oxygen*; LA-UR-12-22377; Los Alamos National Laboratory: Los Alamos, NM, 2012.
8. Worl, L., Berg, John, Bielinberg, Patricia, Carrillo, Alex, Martinez, Max, Montoya, Adam, Veirs, Kirk, Puglisi, Charles, Rademacher, Dave, Schwartz, Dan, Harradine, David, McInroy, Rhonda, Hill, Dallas, Prenger, Coyne, Steward, Jim *Shelf Life Surveillance for PuO2 Bearing Materials FY04 Second Quarterly Report*; LA-UR-04-4228; Los Alamos National Laboratory: 2004.
9. Sims, H. E.; Webb, K. J.; Brown, J.; Morris, D.; Taylor, R. J., Hydrogen yields from water on the surface of plutonium dioxide. *Journal of Nuclear Materials* **2013,** *437* (1-3), 359-364.
10. Brunauer, S.; Emmett, P. H.; Teller, E., Adsorption of Gases in Multimolecular Layers. *Journal of the American Chemical Society* **1938,** *60*.
11. Haschke, J. M.; Ricketts, T. E., Adsorption of water on plutonium dioxide. *Journal of Alloys and Compounds* **1997,** *252*, 148-156.
12. (a) Haschke, J. M.; Allen, T. H.; Morales, L. A., Reaction of Plutonium Dioxide with Water: Formation and Properties of PuO_{2+x}. *Science* **2000,** *287*, 285-286; (b) Haschke, J. M.; Allen, T. H.; Morales, L. A., Reactions of plutonium dioxide with water and hydrogen–oxygen mixtures: Mechanisms for corrosion of uranium and plutonium. *Journal of Alloys and Compounds* **2001,** *314*, 78-91.

Appendix 1: Gas Generation Partial Pressure Data and Uncertainties in kPa

(Page 1 of 1)

Note: Total pressure values used to determine partial pressures were reduced by 4kPa to correct for the estimated partial pressure of water vapor. Partial pressures were corrected for variation in the sensitivity of the GC with time. The average manifold background pressure was subtracted from the partial pressures.

Date	1/15/2004	2/11/2004	6/9/2004	1/24/2005	8/23/2005	4/19/2006	10/23/2006	10/31/2007
Days	38.0	65.0	184.0	413.0	624.0	863.0	1050.0	1423.0
CO_2	0.01	1.45	9.99	19.81	24.86	25.76	27.00	28.78
N_2O	0.01	0.18	1.40	0.72	0.13	0.01	0.03	0.01
He	73.73	75.08	75.58	74.48	70.55	71.20	69.43	68.08
H_2	0.00	0.01	0.81	1.02	0.56	0.27	0.17	0.14
O_2	1.17	0.06	0.07	0.01	0.01	0.01	0.03	0.34
N_2	3.94	3.81	4.82	5.59	6.15	6.42	6.76	8.04
CH_4	0.00	0.00	0.10	0.00	0.00	0.00	0.00	0.00
CO	0.01	0.48	2.45	2.99	6.49	5.78	4.85	3.49

Uncertainties (kPa)

Date	1/15/2004	2/11/2004	6/9/2004	1/24/2005	8/23/2005	4/19/2006	10/23/2006	10/31/2007
CO_2	0.00	0.05	0.24	0.45	0.55	0.57	0.59	0.63
N_2O	0.00	0.02	0.05	0.03	0.01	0.00	0.01	0.00
He	1.52	1.55	1.56	1.56	1.45	1.47	1.43	1.40
H_2	0.00	0.00	0.02	0.03	0.02	0.01	0.01	0.01
O_2	0.04	0.01	0.01	0.00	0.00	0.00	0.01	0.02
N_2	0.11	0.10	0.13	0.15	0.16	0.16	0.17	0.20
CH_4	0.00	0.00	0.01	0.02	0.00	0.00	0.00	0.00
CO	0.00	0.03	0.08	0.00	0.17	0.15	0.13	0.10

Appendix 2: Gas Generation: Total Pressure

(Page 1 of 4)

Date	Pressure (kPa)	Date	Pressure (kPa)	Date	Pressure (kPa)	Date	Pressure (kPa)	Date	Pressure (kPa)
		4/5/2004	91.7	8/16/2004	103.2	12/20/2004	108.7	4/25/2005	111.3
		4/12/2004	93.1	8/23/2004	103.6	12/27/2004	109.1	5/2/2005	111.6
		4/19/2004	92.6	8/30/2004	103.8	1/3/2005	109.3	5/9/2005	111.5
		4/26/2004	92.9	9/6/2004	104.0	1/10/2005	109.3	5/16/2005	111.5
		5/3/2004	94.8	9/13/2004	104.5	1/17/2005	109.5	5/23/2005	111.6
		5/10/2004	95.7	9/20/2004	104.7	1/24/2005	109.8	5/30/2005	111.8
1/12/2004	83.2	5/17/2004	97.2	9/27/2004	105.1	1/31/2005	108.4	6/6/2005	111.9636
1/19/2004	77.5	5/24/2004	97.9	10/4/2004	105.3	2/7/2005	109.2	6/13/2005	112.0231
1/26/2004	78.4	5/31/2004	96.5	10/11/2004	106.0	2/14/2005	109.5	6/20/2005	112.2037
2/2/2004	84.1	6/7/2004	99.7	10/18/2004	106.3	2/21/2005	110.0	6/27/2005	112.5853
2/9/2004	85.0	6/14/2004	98.8	10/25/2004	106.5	2/28/2005	110.0	7/4/2005	112.9358
2/16/2004	85.3	6/21/2004	99.6	11/1/2004	106.9	3/7/2005	110.3	7/11/2005	112.5051
2/23/2004	86.7	6/28/2004	100.3	11/8/2004	107.2	3/14/2005	110.6	7/18/2005	112.2837
3/1/2004	87.5	7/5/2004	100.9	11/15/2004	107.4	3/21/2005	110.7	7/25/2005	112.4994
3/8/2004	88.2	7/12/2004	101.3	11/22/2004	107.1	3/28/2005	110.9	8/1/2005	112.7251
3/15/2004	89.6	7/19/2004	101.8	11/29/2004	107.8	4/4/2005	111.0	8/8/2005	112.8936
3/22/2004	91.4	7/26/2004	102.0	12/6/2004	108.2	4/11/2005	111.2	8/15/2005	112.8578
3/29/2004	90.9	8/2/2004	102.5	12/13/2004	108.5	4/18/2005	111.3	8/22/2005	113.2877

Appendix 2: Gas Generation: Total Pressure

(Page 2 of 4)

Date	Pressure (kPa)	Date	Pressure (kPa)	Date	Pressure (kPa)	Date	Pressure (kPa)	Date	Pressure (kPa)
8/29/2005	112.0153	1/2/2006	113.05	5/8/2006	112.92	9/11/2006	113.11	1/15/2007	112.5402
9/5/2005	112.5563	1/9/2006	113.12	5/15/2006	113.17	9/18/2006	113.12	1/22/2007	112.6828
9/12/2005	112.6474	1/16/2006	113.12	5/22/2006	113.35	9/25/2006	113.18	1/29/2007	113.1026
9/19/2005	112.5455	1/23/2006	113.49	5/29/2006		10/2/2006	113.35	2/5/2007	113.0234
9/26/2005	112.5816	1/30/2006	113.26	6/5/2006	112.89	10/9/2006	113.35	2/12/2007	113.1071
10/3/2005	112.7754	2/6/2006	113.50	6/12/2006	113.06	10/16/2006	114.06	2/19/2007	113.158
10/10/2005	112.70	2/13/2006	113.45	6/19/2006	113.21	10/23/2006	112.9199	2/26/2007	113.5292
10/17/2005	112.55	2/20/2006	113.79	6/26/2006	113.14	10/30/2006	112.8355	3/5/2007	113.4969
10/24/2005	112.64	2/27/2006		7/3/2006	112.94	11/6/2006	113.0179	3/12/2007	113.6118
10/31/2005	112.46	3/6/2006		7/10/2006	112.93	11/13/2006	101.6812	3/19/2007	113.439
11/7/2005	113.02	3/13/2006		7/17/2006		11/20/2006	112.5514	3/26/2007	113.4396
11/14/2005	112.65	3/20/2006		7/24/2006	113.18	11/27/2006	112.8706	4/2/2007	113.5181
11/21/2005	112.52	3/27/2006		7/31/2006	113.09	12/4/2006	112.7586	4/9/2007	113.6053
11/28/2005	112.51	4/3/2006		8/7/2006	113.05	12/11/2006	112.6882	4/16/2007	113.5366
12/5/2005	112.53	4/10/2006	113.92	8/14/2006	113.54	12/18/2006	112.7181	4/23/2007	113.8057
12/12/2005	112.57	4/17/2006	113.88	8/21/2006	113.06	12/25/2006	112.7533	4/30/2007	113.9035
12/19/2005	112.73	4/24/2006	112.93	8/28/2006	113.09	1/1/2007	112.6967	5/7/2007	114.0669
12/26/2005	112.76	5/1/2006	112.79	9/4/2006	113.01	1/8/2007	112.7926	5/14/2007	114.083

Appendix 2: Gas Generation: Total Pressure

(Page 3 of 4)

Date	Pressure (kPa)	Date	Pressure (kPa)
5/21/2007	114.0852	9/24/2007	114.65
5/28/2007	114.0772	10/1/2007	114.44
6/4/2007	114.2024	10/8/2007	114.12
6/11/2007	114.1666	10/15/2007	114.72
6/18/2007	114.3716	10/22/2007	114.91
6/25/2007	114.6025	10/29/2007	114.67
7/2/2007	114.5858	11/5/2007	112.86
7/9/2007	114.7007	11/12/2007	
7/16/2007	114.644	11/19/2007	
7/23/2007	114.5112	11/26/2007	
7/30/2007	114.5291	12/3/2007	
8/6/2007	113.76	12/10/2007	
8/13/2007	113.93	12/17/2007	
8/20/2007	114.52	12/24/2007	
8/27/2007	114.54	12/31/2007	
9/3/2007	114.43	1/7/2008	
9/10/2007	114.61	1/14/2008	
9/17/2007	114.81	1/21/2008	

Appendix 2: Gas Generation: Total Pressure

(Page 4 of 4)

Date	Pressure (kPa)	Date	Pressure (kPa)	Date	Pressure (kPa)	Date	Pressure (kPa)	Date	Pressure (kPa)
2/23/2009	118.71	6/29/2009	118.18	11/2/2009	118.42				
3/2/2009	118.37	7/6/2009	117.89	11/9/2009	118.63				
3/9/2009	117.68	7/13/2009	117.94	11/16/2009	118.83				
3/16/2009	117.56	7/20/2009	117.85	11/23/2009	118.65				
3/23/2009	118.49	7/27/2009	117.95	11/30/2009	118.45				
3/30/2009	118.13	8/3/2009	117.68	12/7/2009	118.50				
4/6/2009	117.96	8/10/2009	117.57	12/14/2009	118.30				
4/13/2009	117.82	8/17/2009	117.84	12/21/2009	115.68				
4/20/2009	117.44	8/24/2009	117.73	12/28/2009	115.43				
4/27/2009	117.43	8/31/2009	117.62	1/4/2010	115.24				
5/4/2009	117.60	9/7/2009	117.51	1/11/2010	115.35				
5/11/2009	117.64	9/14/2009	117.53	1/18/2010	115.46				
5/18/2009	117.70	9/21/2009	118.48	1/25/2010	115.37				
5/25/2009	119.97	9/28/2009	118.65	2/1/2010	115.21				
6/1/2009	120.45	10/5/2009	118.62	2/8/2010	115.35				
6/8/2009	120.36	10/12/2009	118.48						
6/15/2009	119.63	10/19/2009	118.39						
6/22/2009	118.26	10/26/2009	118.45						

Appendix 3: Estimating the monolayer coverage

(Page 1 of 1)

Surface Area: The number of monolayers of moisture on the sample surface may be calculated if the mass of moisture or water, the mass of the sample, and the SSA of the sample are known. One approach is to determine the weight percentage for one monolayer of water. The number of monolayers of water can be calculated by dividing the total weight percentage of water (mass of water/mass of the sample) by the weight percentage of one monolayer of water.[11] The weight percentage of one monolayer of water is the product of the weight of water in a monolayer of 1 m^2 and the SSA:

$$\text{wt\% of 1 ML} = 0.00022\ \text{g m}^{-2}\text{ML}^{-1} \text{ x SSA m}^2\ \text{g}^{-1} \text{ x } 100\ \text{wt\%}$$

$$= 0.022\ \text{wt\% ML}^{-1} \text{x SSA.} \qquad \text{Equation A3-1}$$

For the material SCP711-56A with a SSA of 0.24 m^2 g^{-1}, the weight percentage of one monolayer of water is 0.0053 wt% ML^{-1}.

Dividing the weight percentage of water by the weight percentage of water in one monolayer yields the number of monolayers of water. Applying this to the measured weight percentage of water upon loading and unloading results in:

Loading Condition: 0.060 wt% / 0.0053 wt% ML^{-1} = 11 ML

Unloading Condition: 0.035 wt% / 0.0053 wt% ML^{-1} = 6.6 ML

BET Theory:.The number of monolayers can also be estimated based upon the relative humidity in the.container using Brunauer-Emmett-Teller (BET) theory.[10] BET theory is the standard model for quantifying the equilibria between multiple physically adsorbed layers on a surface and the adsorbing species in the gas above the surface. The specific relationship between the RH above a surface and the number of monolyers of weakly bound water on the surface predicted by BET theory is illustrated in Fig. A-1.

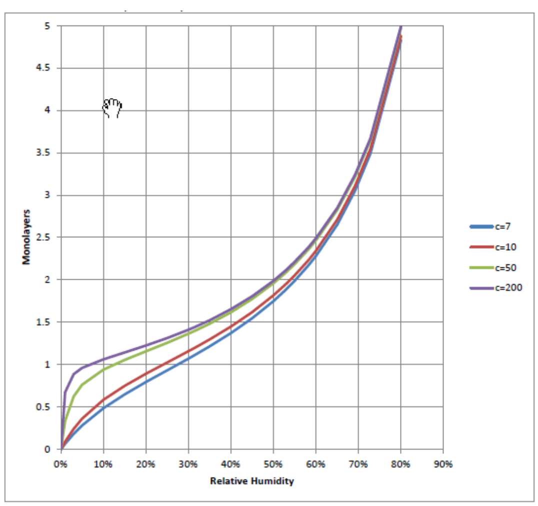

Figure A-1. Adsorption Isotherm Calculated from BET Theory.

Appendix 4: Stopping power ratio

(Page 1 of 1)

The ratio of the stopping power due to the water and the stopping power due to the material is calculated using the approach in Appendix B of Reference 6. Elements with greater than 0.3 wt% were included.

Element or Compound	Integrated Stopping Power from 0 to 5.2 MeV (mg^{-1} cm^{-2})	Elemental Mass Fraction	Elemental Stopping Power (mg^{-1} cm^{-2})
H2O(g)	7.946	0.0000	0
H2O (l)	7.708	0.0067	0.05164
F	6.645	0.0000	0.0000
O	5.901	0.0248	0.1465
Na	5.304	0.0028	0.0147
C	5.190	0.0041	0.0213
S	5.117	0.0000	0.0000
Mg	5.100	0.0002	0.0012
Si	4.852	0.0067	0.0326
Al	4.702	0.0009	0.0042
K	4.652	0.0004	0.0017
Cl	4.575	0.0001	0.0005
Ca	4.461	0.0009	0.0041
Cr	3.688	0.0000	0.0000
Fe	3.504	0.0005	0.0017
Ni	3.184	0.0019	0.0062
Cu	2.871	0.0000	0.0000
Zn	2.860	0.0000	0.0000
Ga	2.786	0.0000	0.0000
UO2	2.081	0.9567	1.9907
PuO2	2.081	0.0000	0.0000
		Smat	2.23
		Swat	7.71
		S	3.46

Appendix 5: Obtaining G-values and rate constants

(Page 1 of 3)

As discussed in the H2 G-value and rate constants section, a double exponential growth function fits the time dependence of the partial pressure curve for hydrogen in many of the MIS studies. The double exponential has three fitting parameters, A0, the initial active water, K1 the hydrogen formation rate constant and K2, the hydrogen consumption rate constant. These fitting parameters can be used along with information of material properties and container geometry to calculate the initial rate, the hydrogen G-value, and empirical rate constants. This appendix documents the methodology for obtaining this information.

Calculation of *$G(H_2)$*

$G(H_2)$ can be calculated by equating the initial rate of hydrogen generation to the product of the rate of dose to the water and *$G(H_2)$*,

$$\frac{dN_{H_2}}{dt} = \dot{D}_{H_2O}\, G(H_2)$$

Equation A5-1

where N_{H2} is the number of molecules of hydrogen and $\dot{D}_{H2O}$ is the rate of adsorbed dose to the water with units eV s^{-1}. The initial rate is given by the differential

$$\frac{dP_{H2}}{dt} = k_1\, A_0 e^{-k_1 t} - k_2 P_{H2}$$

evaluated at time zero in units of molecules per second rather than kPa per day, given P_{H2} is zero at t = 0.

$$\left.\frac{dP}{dt}\right]_{t=0} = k_1\, A_0\, e^{-bt}]_{t=0} = k_1\, A_0$$

$$\frac{dN_{H_2}}{dt} = \frac{dP}{dt}\,\frac{V_g\, N_A}{R\, T} = k_1\, A_0 \frac{V_g\, N_A}{R\, T}\, \frac{day}{86400\, s}$$

$$k_1\, A_0\, \frac{V_g\, N_A}{R\, T}\, \frac{day}{86400\, s} = \dot{D}_{H_2O}\, G(H_2)$$

Equation A5-2

In Equation , V_g is the gas volume within the reactor, N_A is Avogadro's number, *R* is the universal gas constant, *T* is the temperature in the gas phase during the time the data was collected. The method for calculating V_g within an SSR is shown in the Loading section. The dose rate to the water is given by

$$\dot{D}_{H_2O} = P_{mat}\,\frac{6.2418 \text{ x } 10^{18}\text{ eV}}{\text{s W}}\;\; m_{mat}\, f_{H_2O}\,\frac{S_{H_2O}}{S_{mat}}$$

$$f_{H_2O} = \frac{m_{H_2O}}{m_{mat}}$$

$$\dot{D}_{H_2O} = P_{mat}\,\frac{6.2418 \text{ x } 10^{18}\text{ eV}}{\text{s W}}\;\; m_{H_2O}\,\frac{S_{H_2O}}{S_{mat}}$$

Equation A5-3

where P_{mat} is the specific power of the material in W g^{-1}, m_{mat} is the mass of the material, f_{H2O} is the fraction of water, and the ratio S_{H2O}/S_{mat} is the ratio of the stopping power of alpha particles in water to the stopping power in the material. An approach for calculating S_{H2O}/S_{mat} is given in Appendix B. For high-purity plutonium dioxide with adsorbed water and no impurities the ratio S_{H2O}/S_{mat} for 5.2 MeV α-particles is ~3.70. Combining Equation and Equation yields a general expression for $G(H_2)$ using the fitting parameters a and b, and the material properties,

$$G(H_2) = k_1\, A_0\,\frac{V_g N_A}{R\,T}\,\frac{day}{86400\,s}\,\frac{1}{P_{mat}\,\dfrac{6.2418 \text{ x } 10^{18}\text{ eV}/100}{\text{s W}}\;\; m_{H_2O}}\,\frac{1}{\dfrac{S_{H_2O}}{S_{mat}}}$$

Equation A5-4

Conversion of rate constants

The initial formation rate constant, $\boldsymbol{k_{for}}$, can be expressed in terms of molecules of hydrogen produced per second of active water using the equations below.

$$k_{for} = k_1 A_0\,\frac{V_g N_A}{R\,T}\,\frac{day}{86400\,s}$$

Equation A5-5

The consumption rate constant, k_2, expressed in units of days^{-1}, can be expressed in terms of molecules of hydrogen consumed per second per kPa of hydrogen using the equations below.

$$k_{con} = k_2\,\frac{V_g N_A}{R\,T}\,\frac{day}{86400\,s}$$

Equation A5-6

Calculation of rate constants for surface catalyzed decomposition of water to form H_2

The surface catalyzed decomposition of water to form H_2 has been proposed by Haschke and co-workers.[12] The reaction is described by,

$$\mathrm{PuO_2(s)} + x\mathrm{H_2O(ads.)} \longrightarrow \mathrm{PuO_{2+x}(s)} + x\,\mathrm{H_2(g)}$$

Equation A5-7

The reaction "contributes to H_2 pressurization of sealed storage containers until the equilibrium pressure of Equation A5-7 is reached."[12a] The amount of solid plutonium dioxide and water is large compared to the amount of H_2 and higher oxide produced. The initial reaction rate will be essentially constant throughout the reaction. The H_2 consumption reaction, in this case a true back reaction, is first order in H_2 partial pressure and in the amount of the higher oxide. The rate was found to be independent of adsorbed water over a wide range of adsorbed water. The observed initial rate of formation is divided by the total surface area of the material to obtain values that can be compared to Haschke's reaction rates,

$$\mathrm{R_{for}} = A_0 k_1 \frac{day}{24\ hr} \frac{V_g}{R\,T} \frac{1}{SSA\ m_{mat}}$$

Equation A5-8,

where *SSA* is the specific surface area of the material and m_{mat}.is the mass of the plutonium dioxide. This formation rate, $\mathrm{R_{for}}$, is expressed in units of moles m^{-2} hr^{-1} kPa^{-1} of active water. The rate of the surface catalyzed consumption reaction is given by

$$\mathrm{R_{con}} = k_2 \frac{day}{24\ hr} \frac{V_g}{R\,T} \frac{1}{SSA\ m_{mat}}$$

Equation A5-9.

Appendix 6: Symbols and Conversion Factors

(Page 1 of 2)

Symbols

Symbol	Units	Description
A	kPa	Active water or the water involved in hydrogen generation
A_0	kPa	Initial active water (fitting parameter)
k_1	day^{-1}	Rate constant for the formation of hydrogen from water (fitting parameter)
k_2	day^{-1}	Rate constant for the consumption of hydrogen (fitting parameter)
$\dot{D}_x$	$eV\ s^{-1}$ or $J\ s^{-1}$ or W	Rate of adsorbed dose to x
$G(x)$	molecules 100 eV^{-1}	Number of molecules of x produced per 100 eV of adsorbed dose
f_x	---	Fraction of material x in the total material
m_x	g	Mass of x
N_x	molecules	Number of molecules of substance x
N_A	molecules mol^{-1}	Avogadros number
p_x	kPa	Partial pressure of x
P_x	$W\ g^{-1}$ or $eV\ s^{-1}\ g^{-1}$	Specific power of x
S_x	m	Stopping power of x to alpha radiation
SSA	$m^2\ g^{-1}$	Specific Surface Area of the material
t	s or day or yr	Time
T	K	Temperature
V_g	cm^3	Volume that the gas occupies

Appendix 6: Symbols and Conversion Factors

(Page 2 of 2)

Unit conversions

1 W	6.2418 x 10^{18} eV s^{-1}
1 day	86400 s
1 day	24 hr
N_A	6.0221367x10^{23} molecules mol^{-1}
R	8.314510 J mol^{-1} K^{-1} 8.314510 kPa L mol^{-1} K^{-1} 8314.510 kPa cm^3 mol^{-1} K^{-1}